Fulde-Ferrell-Larkin-Ovchinnikov state in spin-orbit-coupled superconductors

F. Yang and M. W. Wu*

Hefei National Laboratory for Physical Sciences at Microscale, Department of Physics, and CAS Key Laboratory of Strongly-Coupled Quantum Matter Physics, University of Science and Technology of China, Hefei, Anhui, 230026, China

(Dated: April 4, 2017)

We show that in the presence of magnetic field, two superconducting phases with the center-of-mass momentum of Cooper pair parallel to the magnetic field are induced in spin-orbit-coupled superconductor Li_2Pd_3B. Specifically, at small magnetic field, the center-of-mass momentum is induced due to the energy-spectrum distortion and no unpairing region with vanishing singlet correlation appears. We refer to this superconducting state as the drift-BCS state. By further increasing the magnetic field, the superconducting state falls into the Fulde-Ferrell-Larkin-Ovchinnikov state with the emergence of the unpairing regions. The observed abrupt enhancement of the center-of-mass momenta and suppression on the order parameters during the crossover indicate the first-order phase transition. Enhanced Pauli limit and hence enlarged magnetic-field regime of the Fulde-Ferrell-Larkin-Ovchinnikov state, due to the spin-flip terms of the spin-orbit coupling, are revealed. We also address the triplet correlations induced by the spin-orbit coupling, and show that the Cooper-pair spin polarizations, generated by the magnetic field and center-of-mass momentum with the triplet correlations, exhibit totally different magnetic-field dependences between the drift-BCS and Fulde-Ferrell-Larkin-Ovchinnikov states.

PACS numbers: 74.25.-q, 71.70.Ej, 74.81.-g, 74.25.Dw

arXiv:1704.00409v1 [cond-mat.supr-con] 3 Apr 2017

I. INTRODUCTION

Ever since the Bardeen, Cooper and Schrieffer (BCS) mechanism of superconductivity was proposed,[1] it is well established that the Cooper pair in conventional superconductors such as Al, Pb and Nb, is formed by two electrons with opposite momenta and spins near the Fermi surface. Together with the conventional s-wave attractive potential, spatially uniform singlet order parameter is realized. After that, possibility of unconventional Cooper pairing together with the corresponding nontrivial superconductivity has attracted much attention. Specifically, in spin space, from the symmetry analysis, triplet superconductivity with Cooper pair formed by electrons with the same spin and opposite momenta is theoretically revealed in systems with the broken space-inversion symmetry.[2–12] Recently, this possibility has been primarily realized in noncentrosymmetric superconducting material Sr_2RuO_4,[13–20] and the ongoing experimental evidence makes such material a promising candidate to realize non-dissipative spin transport and hence spintronic application.[21–30]

With attention attracted to the orbital degree of freedom of the pairing, another class of unconventional superconducting state, characterized by singlet Cooper pairs with a finite center-of-mass (CM) momentum, is expected at large magnetic field. This was first predicted by Fulde and Ferrell (FF)[31] and a little later by Larkin and Ovchinnikov (LO)[32] independently in 1960s. Specifically, the presence of the magnetic field leads to the mismatched Fermi surfaces for spin-up and -down electrons, and consequently, near the corresponding Fermi surfaces, there exist unpairing regions in which the electron can not find the pairing partner with opposite momentum and spin to form into a Cooper pair. Particularly, when the magnetic field exceeds a critical strength, by inducing a finite CM momentum of the Cooper pair, the magnitudes and orientations of the momenta between the pairing electrons can both be different. Then, the pairing region between the spin-up and -down electrons is maximized, leading to the free energy minimized. In this situation, with the rotational symmetry of the system with respect to the CM-momentum orientation, FF proposed an order-parameter $\Delta(\mathbf{r}) = \Delta_0 e^{i\mathbf{q}\cdot\mathbf{r}}$ with the inhomogeneously broadened phase but spatially uniform amplitude[31] whereas LO referred to another order-parameter $\Delta(\mathbf{r}) = \Delta_0 \cos(\mathbf{q}\cdot\mathbf{r})$ which shows the uniform phase but spatially nonuniform amplitude.[32] These two types of the order parameters, now both referred to as the FFLO state,[33,34] have attracted tremendous theoretical and experimental efforts for decades to prove their existence. Examples include superconducting heavy fermion[35–43] and ultracold atom[44–52] systems, multi-band Fe-based superconductors[53–56] as well as the organic superconductors.[57–64] However, up till now, the conclusive experimental evidence is still missing.

The experimental difficulty arises from several different aspects. Specifically, from the FFLO theory, the FFLO state occurs in a very narrow magnetic-field regime,[31,33,34] leading to the stringent experimental requirement. The unavoidable disorder in systems may also destroy the induced CM momentum of Cooper pair and hence the FFLO state.[42,65,66] Moreover, in most superconducting materials, the destruction of superconductivity comes from the orbital effect of the magnetic field.[33,34,67,68] Weak orbital depairing effect of the magnetic field is required so that the superconductivity can survive the transition from the BCS state

into the FFLO one. Consequently, very few superconducting materials have been found as possible candidates for the occurrence of the FFLO state, such as superconducting heavy fermion material[35–43] and organic superconductors[57–64] mentioned above. Particularly, a magnetic-field-induced superconducting phase in heavy-fermion compound $CeCoIn_5$ was reported from the thermodynamic experiments,[35–40] which is claimed to be the FFLO state and more microscopic experimental confirmation is still in progress.

Furthermore, it is reported that the anisotropic Fermi surface is favorable for the stability of the FFLO state.[69] After that, the spin-orbit-coupled superconductors attract much attention, since the interplay between the spin-orbit coupling (SOC)[70–72] and magnetic field can lead to a marked mismatch of the energy spectra between spin-up and -down electrons as well as the Fermi surfaces.[73] During the last several years, there indeed have been several theoretical reports in spin-orbit-coupled ultracold atomic gases[74–81] and indirect experimental evidences from superconducting systems with SOC[82–85] indicating the existence for the FFLO state by the magnetic field. Specifically, with SOC and magnetic field, the FFLO state with induced CM momentum is theoretically predicted by Zheng *et al.*.[74] Enlarged magnetic-field regime of the FFLO state due to the enhanced Pauli limit is also revealed in their work, in accord with the experiments.[82–85] After that, according to the quasiparticle energy spectra, the FFLO state with SOC is further divided into gapped and gapless ones, which occur at small and large magnetic fields, respectively.[75–78] Moreover, it is also reported that the magnetic field and SOC break the rotational symmetry with respect to the CM-momentum orientation, and then CM momenta parallel[75] and perpendicular[81] to the magnetic field are predicted in the FFLO states with Dresselhaus and Rashba SOCs, respectively. Furthermore, by the determined CM-momentum orientation, it is proposed[80] that the FF phase can be enhanced over the LO one. However, the theoretical works above are based on the numerical calculation of the free-energy minimum with respect to CM momentum and order parameter, since it is difficult to directly obtain the gap equation by analytically diagonalizing Hamiltonian with SOC. Therefore, with the numerical difficulty from multi-variable minimum problem, specific behaviors of the superconducting state around phase transition are unclear in the literature. The pairing mechanism and microscopic properties including singlet correlation are also beyond this method. Particularly, study of the unpairing regions with vanishing singlet correlation, which are the hallmark of the FFLO state,[31] is still absent.

In this work, we systematically investigate the properties of the FFLO state with an induced CM momentum in the spin-orbit-coupled superconductors with the magnetic field. Specifically, by analytically obtaining the anomalous Green function, we derive the singlet correlation and hence the gap equation. Then, by self-consistently solving the gap equation, the superconducting state and its corresponding properties can be determined by numerically calculating the energy minimum with respect to a single parameter, i.e., the CM momentum. We further carry out the numerical calculation in superconductor Li_2Pd_3B[86–91] where strong Dresselhaus SOC[87,88] and conventional BCS superconductivity at zero magnetic field[86,90,91] are realized.

The calculation shows that with the SOC, the CM momentum parallel to the magnetic field is induced at small field, similar to the gapped FFLO state mentioned above.[75–78] Nevertheless, with an induced CM momentum in this case, no unpairing region with vanishing singlet correlation is developed. This is very different from the conventional FFLO state without SOC, where the CM momentum is induced simultaneously with the emergence of the unpairing regions.[31] By looking into the pairing mechanism, it is further shown that the induced CM momentum with SOC at small magnetic field is due to the energy-spectrum distortion, resembling the intravalley pairing in graphene[92] and transition metal dichalcogenides,[93] and hence has different origin from the case in conventional FFLO state.[31] Therefore, it is more appropriate to refer to such superconducting state, in which the CM momentum of the Cooper pair is induced but no unpairing region is developed, as the drift-BCS state. By further increasing the magnetic field, abrupt enhancement of the CM momenta and suppression on the order parameters are observed, meaning the occurrence of the first-order phase transition. Particularly, after the transition, we find that unpairing regions with vanishing singlet correlation are induced, indicating the emergence of the FFLO state, resembling the conventional FFLO one.[31] We show that the emerged FFLO state here corresponds to the gapless one mentioned above.[75–78] Enhanced Pauli limit and hence enlarged magnetic-field regime of the emerged FFLO state by SOC are also observed in our work. We further show that the enhancement of the Pauli limit is due to the spin-flip terms of the SOC, which suppress the unpairing regions. Finally, we discuss the triplet correlations induced by the SOC,[4,7,11,12] and show that the Cooper-pair spin polarizations,[2,3,94,95] which are predicted to be induced by magnetic field and CM momentum in the presence of triplet correlations,[95] exhibit totally different magnetic-field dependences between the drift-BCS and FFLO states. This provides an experimental scheme to distinguish these two phases through the reported magnetoelectric Andreev effect,[94–96] in addition to the phase transition.

This paper is organized as follows. In Sec. II, we introduce our model and present the calculation of the energy for superconducting state. The specific numerical results in Li_2Pd_3B and analytic analysis are presented in Sec. III. We summarize in Sec. IV.

II. MODEL

In this section, we first present the Hamiltonian of the spin-orbit coupled s-wave superconductor in the presence of the magnetic field. Then we give the gap equation and lay out the calculation of the energy for the superconducting state.

A. HAMILTONIAN AND GAP EQUATION

With the magnetic field and CM momentum of Cooper pair, by defining the Nambu spinors $\hat{\Phi}_{\mathbf{k}} = [\phi_{\uparrow\mathbf{k}+\mathbf{q}}, \phi_{\downarrow\mathbf{k}+\mathbf{q}}, \phi^{\dagger}_{\uparrow-\mathbf{k}+\mathbf{q}}, \phi^{\dagger}_{\downarrow-\mathbf{k}+\mathbf{q}}]^T$, we present the Hamiltonian H_S of the spin-orbit-coupled s-wave superconductor as:[12,31,95]

$$\hat{H}_S = \frac{1}{2}\int d\mathbf{k}\hat{\Phi}^{\dagger}_{\mathbf{k}}\hat{H}_s(\mathbf{k})\rho_3\hat{\Phi}_{\mathbf{k}}, \tag{1}$$

with

$$\hat{H}_s(\mathbf{k}) = \begin{pmatrix} \xi_{\mathbf{k}^+} + \mathbf{\Omega}_{\mathbf{k}^+}\cdot\boldsymbol{\sigma} & \Delta_{\mathbf{q}} i\sigma_2 \\ \Delta^*_{\mathbf{q}} i\sigma_2 & \xi_{\mathbf{k}^-} + \mathbf{\Omega}_{\mathbf{k}^-}\cdot\boldsymbol{\sigma} \end{pmatrix}. \tag{2}$$

Here, $\rho_3 = \sigma_0 \otimes \tau_3$; σ_i and τ_i stand for the Pauli matrices in spin and particle-hole spaces, respectively; $\mathbf{k}^{\pm} = \pm\mathbf{k} + \mathbf{q}$ with $\mathbf{q}$ standing for the CM momentum; $\xi_{\mathbf{k}} = \varepsilon_{\mathbf{k}} - E_F$ and $\varepsilon_{\mathbf{k}} = k^2/(2m^*)$ with m^* being the effective mass of electrons in superconductor and E_F denoting the Fermi energy; $\mathbf{\Omega}_{\mathbf{k}} = \mathbf{h}_{\mathbf{k}} + \mathbf{h}_B$ with $\mathbf{h}_{\mathbf{k}}$ and $\mathbf{h}_B$ representing the SOC and Zeeman energy, respectively; $\Delta_{\mathbf{q}} = -V\sum'_{\mathbf{k}}\langle\phi_{\uparrow\mathbf{k}+\mathbf{q}}\phi_{\downarrow-\mathbf{k}+\mathbf{q}}\rangle$ stands for the order parameter of the superconducting state in the momentum space; $\langle\ \rangle$ stands for the ensemble average; V is the conventional s-wave attractive potential in superconductors. It is noted that the order parameter at this case can be transformed into the FF form[31] $\Delta(\mathbf{r}) = \Delta_{\mathbf{q}}e^{i\mathbf{q}\cdot\mathbf{r}}$ in real space.

In Nambu⊗spin space, the equilibrium Green function[97–99] in the momentum space is given by

$$G_{\mathbf{q}}(\mathbf{k},\tau) = -\rho_3\langle T_\tau\hat{\Phi}_{\mathbf{k}}(\tau)\hat{\Phi}^{\dagger}_{\mathbf{k}}(0)\rangle, \tag{3}$$

where T_τ represents the chronological-ordering operator; τ is the imaginary time. By expressing

$$G_{\mathbf{q}}(\mathbf{k},\tau) = \begin{pmatrix} g_{\mathbf{q}}(\mathbf{k},\tau) & f_{\mathbf{q}}(\mathbf{k},\tau) \\ f^{\dagger}_{\mathbf{q}}(-\mathbf{k},\tau) & g^{\dagger}{}_{\mathbf{q}}(-\mathbf{k},\tau) \end{pmatrix}, \tag{4}$$

one can obtain the normal Green function $g_{\mathbf{q}}(\mathbf{k},\tau)$ and anomalous Green function $f_{\mathbf{q}}(\mathbf{k},\tau)$.[4,97–99]

Then, in the Matsubara representation[97–99] $G_{\mathbf{k}}(i\omega_n) = \int_0^\beta d\tau e^{i\omega_n\tau}G_{\mathbf{k}}(\tau)$, from the Gor'kov equation:[100]

$$[i\omega_n\rho_3 - H_s(\mathbf{k})]G_{\mathbf{q}}(\mathbf{k},i\omega_n) = 1, \tag{5}$$

one has

$$(i\omega_n - \xi_{\mathbf{k}^+} - \mathbf{\Omega}_{\mathbf{k}^+}\cdot\boldsymbol{\sigma})f_{\mathbf{q}}(\mathbf{k},i\omega_n) - \Delta_{\mathbf{q}}i\sigma_2 g^{\dagger}_{\mathbf{q}}(\mathbf{k},i\omega_n) = 0, \tag{6}$$

$$-\Delta^*_{\mathbf{q}}i\sigma_2 f_{\mathbf{q}}(\mathbf{k},i\omega_n) + (i\omega_n - \xi_{\mathbf{k}^-} - \mathbf{\Omega}_{\mathbf{k}^-}\cdot\boldsymbol{\sigma})g^{\dagger}_{\mathbf{q}}(\mathbf{k},i\omega_n) = 1. \tag{7}$$

Here, $\beta = 1/(k_BT)$ with k_B being the Boltzmann constant and T representing the temperature; $\omega_n = (2n+1)\pi k_BT$ are the Matsubara frequencies with n being integer.

Following the previous work,[95] through multiplying Eq. (7) by $i\sigma_2$ from the left side, one immediately has

$$\Delta^*_{\mathbf{q}}f_{\mathbf{q}}(\mathbf{k},i\omega_n) + (i\omega_n - \xi_{\mathbf{k}^-} + \mathbf{\Omega}_{\mathbf{k}^-}\cdot\boldsymbol{\sigma}^*)i\sigma_2 g^{\dagger}_{\mathbf{q}}(\mathbf{k},i\omega_n) = i\sigma_2. \tag{8}$$

Then, by using Eq. (6) to replace $i\sigma_2 g^{\dagger}_{\mathbf{q}}(\mathbf{k},i\omega_n)$ in Eq. (8), the anomalous Green function can be obtained:

$$f_{\mathbf{q}}(\mathbf{k},i\omega_n) = [f^s_{\mathbf{q}}(\mathbf{k},i\omega_n) + \mathbf{f}^t_{\mathbf{q}}(\mathbf{k},i\omega_n)\cdot\boldsymbol{\sigma}]i\sigma_2, \tag{9}$$

with the singlet $f^s_{\mathbf{q}}(\mathbf{k},i\omega_n)$ and triplet $\mathbf{f}^t_{\mathbf{q}}(\mathbf{k},i\omega_n) = (\frac{f_{\downarrow\downarrow}-f_{\uparrow\uparrow}}{2}, \frac{f_{\downarrow\downarrow}+f_{\uparrow\uparrow}}{2i}, f_{\downarrow\uparrow+\uparrow\downarrow})$ pairings[101,102] written as:

$$\begin{aligned} f^s_{\mathbf{q}}(\mathbf{k},i\omega_n) &= \frac{\Delta_{\mathbf{q}}}{w_{\mathbf{q}}(\mathbf{k},i\omega_n)}[(i\omega_n - \xi_{\mathbf{k}^+})(i\omega_n + \xi_{\mathbf{k}^-}) \\ &\quad + \mathbf{\Omega}_{\mathbf{k}^+}\cdot\mathbf{\Omega}_{\mathbf{k}^-} - |\Delta_{\mathbf{q}}|^2], \end{aligned} \tag{10}$$

$$\begin{aligned} \mathbf{f}^t_{\mathbf{q}}(\mathbf{k},i\omega_n) &= \frac{\Delta_{\mathbf{q}}}{w_{\mathbf{q}}(\mathbf{k},i\omega_n)}[(i\omega_n - \xi_{\mathbf{k}^+})\mathbf{\Omega}_{\mathbf{k}^-} + (i\omega_n \\ &\quad + \xi_{\mathbf{k}^-})\mathbf{\Omega}_{\mathbf{k}^+} - i\mathbf{\Omega}_{\mathbf{k}^+}\times\mathbf{\Omega}_{\mathbf{k}^-}], \end{aligned} \tag{11}$$

$$w_{\mathbf{q}}(\mathbf{k},i\omega_n) = \prod_{\mu=\pm}(i\omega_n - E^e_{\mu\mathbf{k}})(i\omega_n - E^h_{\mu\mathbf{k}}). \tag{12}$$

$E^{e(h)}_{\mu\mathbf{k}}$ ($\mu = \pm$) stand for the quasiparticle electron (hole) energy spectra in superconductors, which can be obtained from the solutions of equation $|f^s_{\mathbf{q}}(\mathbf{k},\omega)|^2 - |\mathbf{f}^{\mathbf{t}}_{\mathbf{q}}(\mathbf{k},i\omega)|^2 = 0$ with respect to ω.

With the anomalous Green function, the singlet $\rho^s_{\mathbf{q}}$ and triplet $\boldsymbol{\rho}^t_{\mathbf{q}} = (\frac{\rho^t_{s=-1}-\rho^t_{s=1}}{2}, \frac{\rho^t_{s=-1}+\rho^t_{s=1}}{2i}, \rho^t_{s=0})$[101–103] correlations are defined as

$$\rho^s_{\mathbf{q}}(\mathbf{k}) = -\frac{1}{\beta}\sum_{i\omega_n} f^s_{\mathbf{q}}(\mathbf{k},i\omega_n), \tag{13}$$

$$\boldsymbol{\rho}^t_{\mathbf{q}}(\mathbf{k}) = -\frac{1}{\beta}\sum_{i\omega_n} \mathbf{f}^t_{\mathbf{q}}(\mathbf{k},i\omega_n). \tag{14}$$

Then one immediately has the gap equation:[100]

$$\Delta_{\mathbf{q}} = V\sum_{\mathbf{k}}{}' \rho^s_{\mathbf{q}}(\mathbf{k}). \tag{15}$$

Here, the summation is taken for the values of $\mathbf{k}$ satisfying $|E_{\uparrow\mathbf{k}} - E_F| < \omega_D$ and $|E_{\downarrow\mathbf{k}} - E_F| < \omega_D$ where $E_{\uparrow(\downarrow)\mathbf{k}}$ is the energy of spin-up (-down) electron with the momentum $\mathbf{k}$; ω_D stands for the Debye frequency. It is noted that due to the conventional s-wave attractive potential, only singlet order parameter exists. Then, by self-consistently solving Eq. (15), the order parameter $\Delta_{\mathbf{q}}$ at fixed CM momentum of Cooper pair $\mathbf{q}$ is obtained.

B. GROUND-STATE ENERGY

Following the previous work by FF,[31] by replacing the s-wave attractive potential V with an effective one λ in Eq. (15), an potential-dependent order parameter $\Delta_{\mathbf{q}}(\lambda)$ can be immediately obtained by self-consistently solving Eq. (15).

Then, by neglecting the Fock energy of the normal state, based on Feynman-Hellmann theorem

$$\partial_\lambda E = \langle \partial_\lambda H_s(\lambda) \rangle = -\frac{|\Delta_{\mathbf{q}}(\lambda)|^2}{\lambda^2}, \tag{16}$$

the expectation value of the energy difference between the superconducting state $E^S_{\mathbf{q}}$ and normal one E^N is given by

$$\delta E_{\mathbf{q}} = E^S_{\mathbf{q}} - E^N = -\int_{V_0}^{V} d\lambda \frac{|\Delta_{\mathbf{q}}(\lambda)|^2}{\lambda^2}, \tag{17}$$

where V_0 is the effective attractive potential at the transition point between the superconducting state and the normal one $[\Delta_{\mathbf{q}}(V_0) = 0]$. Then, by calculating the minimum of $\delta E_{\mathbf{q}}$ with respect to a single parameter, i.e., the CM momentum $\mathbf{q}$, the properties of the superconducting state including the CM momentum, order parameter, quasiparticle energy spectra, singlet and triplet correlations can all be determined. Particularly, it is noted that through self-consistently solving the gap equation in our work, the numerical difficulty from the multi-variable minimum problem mentioned in the introduction is reduced, leading to more accurate results.

TABLE I: Parameters used in our calculation. Note that m_0 stands for the free electron mass. Δ_0 is the order parameter at $T = 0$ K without magnetic field. V is obtained by fitting Δ_0. k_F is the largest momentum with the Fermi energy in the absence of the magnetic field.

m^*/m_0	3.049[a]	E_F (meV)	70[a]
Δ_0 (meV)	1.2732[b]	ω_D (meV)	38.088[b]
γ (meV·Å)	23.28[a]	T (K)	0
V (meV)	0.218	k_F (Å^{-1})	0.246

[a] Refs. 86. [b] Ref. 87.

III. NUMERICAL RESULTS

In this section, by numerically solving Eq. (17), we discuss the properties of the superconducting state in spin-orbit-coupled superconductors. The specific numerical calculation is carried out in the material Li_2Pd_3B,[86–91] in which the conventional s-wave BCS behavior[87,88] and strong SOC[86,90,91] have been realized. The SOC in Li_2Pd_3B has the Dresselhaus form $\mathbf{h_k} = \gamma \mathbf{k}$,[90,91] in consistence with the cubic symmetry. All the material parameters used in our calculation are listed in Table I. The magnetic field is chosen along the z direction.

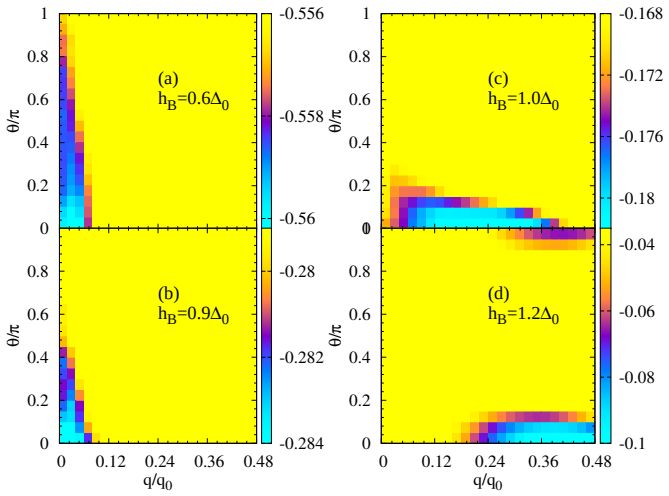

FIG. 1: $\delta E_{\mathbf{q}}$ versus longitude θ (with respect to $\mathbf{h}_B$) and magnitude q of the CM momentum at (a) $h_B = 0.6\Delta_0$, (b) $h_B = 0.9\Delta_0$, (c) $h_B = 1.0\Delta_0$ and (d) $h_B = 1.2\Delta_0$. $q_0 = \sqrt{2m^*(E_F + h_B)} - \sqrt{2m^*(E_F - h_B)}$.

A. Orientation of CM momentum and Pairing Mechanism

We first focus on the CM-momentum dependences of the energy of the superconducting state at different magnetic fields. We find that the energy difference $\delta E_{\mathbf{q}}$ between the superconducting state and normal one always shows isotropy with respect to the latitude of the CM momentum around the magnetic field (not shown). This is due to the spatial-rotational symmetry around the magnetic field of the system. Then, $\delta E_{\mathbf{q}}$ as function of the longitude θ (with respect to the magnetic field) and magnitude q of the CM momentum are plotted in Fig. 1 at different magnetic fields. As seen from the figure, in the presence of the magnetic field, the minimum of $\delta E_{\mathbf{q}}$ is always reached at finite q with $\theta = 0$ (z direction). This indicates that a CM momentum parallel to magnetic field is induced in the superconducting state in the presence of the magnetic field and SOC, similar to the previous work with the same Dresselhaus SOC.[75] Small and large CM momenta are observed before [Figs. 1(a) and (b)] and after [Figs. 1(c) and (d)] $h_B = \Delta_0$ here, respectively. Particularly, with the determined orientation according to the energy minimum, the induced CM momentum is inherently robust against the impurity scattering.

To illustrate the pairing mechanism, we further plot the energy spectra of spin-up and -down electrons along the k_z direction (magnetic-field direction) with and without magnetic field in Fig. 2. As seen from the figure, without the magnetic field, the SOC leads to the opposite shifts of the energy spectra between spin-up (red solid curve) and -down (blue dotted curve) electrons along the k_z direction. Then, the magnetic field causes the opposite energy shifts of the energy spectra between spin-up

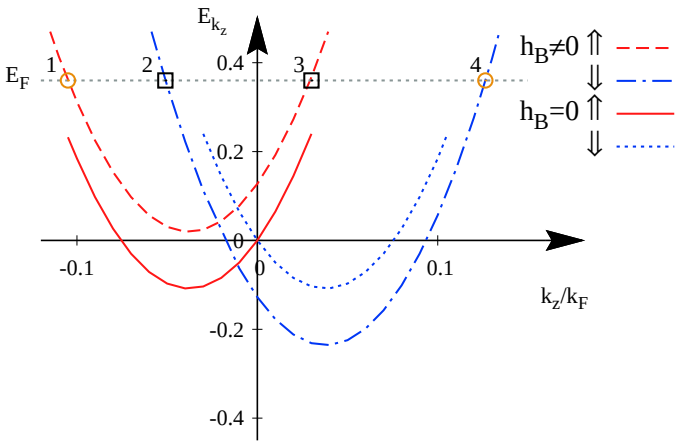

FIG. 2: Energy spectra of spin-up and -down electrons along k_z direction. Dashed and chain curves: SOC and magnetic field are both included; Solid and dotted curves: only SOC in included. The horizontal dotted line indicates the Fermi surface. Circles (Squares): type I (II) pairing formed by spin-up electron 1 (3) and spin-down one 4 (2).

(red dashed curve) and -down (blue chain curve) electrons. In this situation, by assuming the Debye frequency $\omega_D = 0$, the Cooper pairing only occurs at the Fermi surface, as shown in Fig. 2. Then, there exist two possible types of Cooper pairings: type I, formed by spin-up electron 1 (with $-\mathbf{k}_{\rm I}+\mathbf{q}$) and spin-down one 4 (with $\mathbf{k}_{\rm I}+\mathbf{q}$) in Fig. 2 in favor of the CM momentum $\mathbf{q}=q_c\mathbf{z}$ ($q_c = \frac{\sqrt{|m^*\gamma|^2+2m^*(E_F+h_B)}-\sqrt{|m^*\gamma|^2+2m^*(E_F-h_B)}}{2}$); type II, formed by spin-up electron 3 (with $\mathbf{k}_{\rm II}+\mathbf{q}$) and spin-down one 2 (with $-\mathbf{k}_{\rm II}+\mathbf{q}$) in Fig. 2, in favor of the CM momentum $\mathbf{q}=-q_c\mathbf{z}$. Nevertheless, from Fig. 1, the CM momentum $\mathbf{q}$ is along the $\mathbf{z}$ direction, as mentioned above. This indicates the type I pairing makes the leading contribution in the determination of the CM momentum.

The leading role of type I pairing can be understood as follows. On one hand, the relative momentum $k_{\rm I}$ in type I pairing is larger than $k_{\rm II}$ in type II one. Then, with the larger relative momentum k and hence larger density of states in Eq. (15), type I pairing makes the leading contribution to the summation with respect to the momentum space. On other hand, from the framework of the Ginzburg-Landau theory, the free energy densities of superconducting system reads

$$\mathcal{F} = \alpha|\psi(\mathbf{r})|^2 + \frac{\eta}{2}|\psi(\mathbf{r})|^4 + \frac{1}{2m}[\mathbf{\Pi}\psi(\mathbf{r})]^*[\mathbf{\Pi}\psi(\mathbf{r})], \quad (18)$$

with $\mathbf{\Pi} = -i\hbar\mathbf{\nabla} + 2e\mathbf{A}$ and $\psi(\mathbf{r}) = \Delta(\mathbf{r})/V$; α and η being the corresponding expansion parameters; $\mathbf{A}$ standing for the magnetic vector potential. In the presence of the SOC, one can replace $\mathbf{A}$ by $\mathbf{A_s}$ with $\mathbf{A_s}=\gamma\mathbf{s}$ for the Dresselhaus SOC and $\mathbf{s}$ representing the spin vector of electrons. Then, terms related to the SOC in Eq. (18) are written as

$$\begin{aligned}\mathcal{F}_s &= \frac{\mathrm{Re}[\Delta^*(\mathbf{r})2e\mathbf{A}_s\cdot(-i\hbar\mathbf{\nabla})\Delta(\mathbf{r})]}{mV^2} + \frac{e^2|\mathbf{A}_s\Delta(\mathbf{r})|^2}{mV^2} \\ &= \frac{2e\hbar\gamma|\Delta_{\mathbf{q}}|^2}{mV^2}\mathbf{s}\cdot\mathbf{q} + \frac{2e^2\gamma^2|\mathbf{s}\Delta_{\mathbf{q}}|^2}{mV^2}, \end{aligned} \quad (19)$$

where we have applied $\Delta(\mathbf{r}) = \Delta_{\mathbf{q}}e^{i\mathbf{q}\cdot\mathbf{r}}$ in Eq. (19). With the magnetic field, the spin vector $\mathbf{s}$ is anti-parallel to $\mathbf{h}_B$. Hence, to obtain the free-energy minimum, the induced CM momentum $\mathbf{q}$ should be parallel to the magnetic field ($\mathbf{z}$ direction), in accord with the type I pairing (in favor of $\mathbf{q}=q_c\mathbf{z}$).

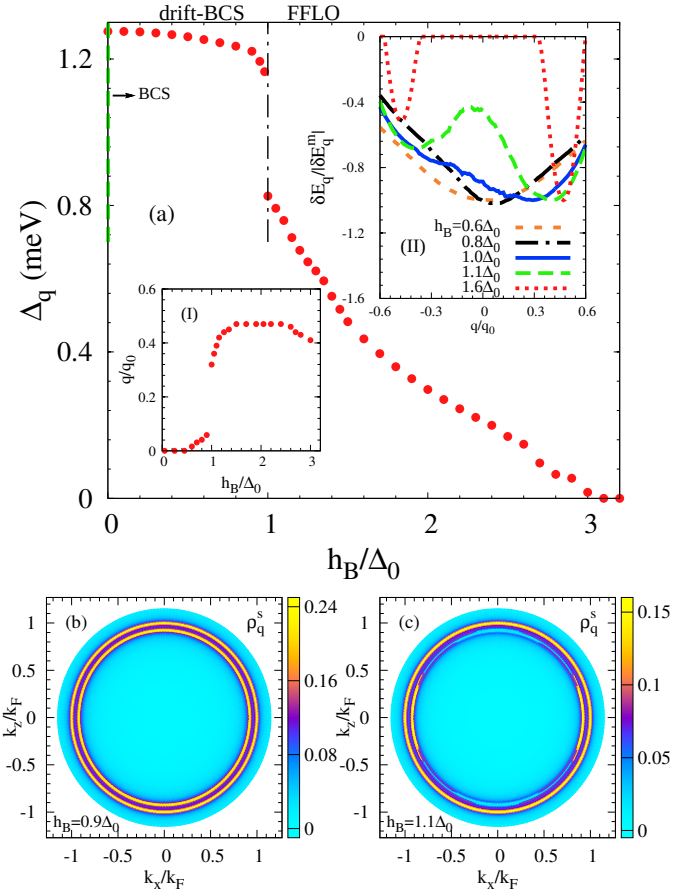

FIG. 3: (a): magnetic-field dependence of $\Delta_{\mathbf{q}}$. The vertical dashed (chain) line indicates the BCS state (crossover between the drift-BCS and FFLO states). The inset (I) in (a) shows the CM momentum as function of magnetic field. The inset (II) in (a) exhibits $\delta E_{\mathbf{q}}$ versus $\mathbf{q}=q\mathbf{z}$ at different magnetic fields. The results in inset (b) is renormalized by the maximum of $|\delta E_{\mathbf{q}}|$ for each magnetic field. $q_0 = \sqrt{2m^*(E_F+h_B)} - \sqrt{2m^*(E_F-h_B)}$. (b) [(c)]: singlet correlations in the momentum space at $h_B = 0.9\Delta_0$ ($h_B = 1.1\Delta_0$).

B. Phase diagram

In this part, we discuss the phase diagram of the superconducting state. The magnetic field dependences of the order parameter $\Delta_{\mathbf{q}}$ and CM momentum $\mathbf{q} = q\mathbf{z}$ are plotted in Fig. 3(a) and the inset (I) of Fig. 3(a), respectively. In the calculation, $\mathbf{q}$ is chosen at the minimum of $\delta E_{\mathbf{q}}$. As seen from Fig. 3(a) and inset (I), with the increase of magnetic field from zero, before reaching $h_B = \Delta_0$, the order parameter decreases slightly [Fig. 3(a)]. In the same time, a CM momentum is induced and increases from zero [inset (I)], similar to the gapped FFLO state in the previous works[75–78] mentioned in the introduction. Nevertheless, by plotting the singlet correlation at $h_B = 0.9\Delta_0$ in Fig. 3(b), it is seen from the figure that two separated and complete circles with finite $\rho^s_{\mathbf{q}}(\mathbf{k})$, corresponding to type I (large k) and II (small k) pairings, are observed due to the presence of the SOC, and no unpairing region with vanishing $\rho^s_{\mathbf{q}}(\mathbf{k})$ appears when $h_B < \Delta_0$. As mentioned in the introduction, it is more appropriate to refer to such superconducting state in which the CM momentum is induced but no unpairing region is observed, as the drift-BCS state, since the induced CM momentum at small magnetic field here arises from the energy-spectrum distortion by the magnetic field and SOC as mentioned in Sec. III A, resembling the intravalley pairing in graphene[92] and transition metal dichalcogenides,[93] and hence has different origin from the case in the conventional FFLO state without SOC.[31]. Particularly, since this drift-BCS state occurs at small magnetic field, it can inherently survive against the orbital depairing effect.

By further increasing the magnetic field, abrupt suppression on the order parameters [shown in Fig. 3(a)] and enhancement of the CM momenta [shown in the inset (I) of Fig. 3(a)] are observed before and after $h_B \approx \Delta_0$, indicating the first-order phase transition at the crossover. The abrupt changes can be understood from the inset (II) of Fig. 3(a) where we plot the energy differences $\delta E_{\mathbf{q}}$ versus $\mathbf{q} = q\mathbf{z}$ at different magnetic fields. From the inset (II), it is seen that when $h_B < \Delta_0$, the minimum of $\delta E_{\mathbf{q}}$ sits near $q \approx 0$ (brown dashed curve), and the minimum position q_m increases with the magnetic field by comparing the brown dashed curve at $h_B = 0.6\Delta_0$ with the black chain one at $h_B = 0.8\Delta_0$. Whereas with the increase of magnetic field when $h_B \geq \Delta_0$, $\delta E_{\mathbf{q}\approx\mathbf{0}}$ increases and then the minimum of $\delta E_{\mathbf{q}}$ appears around $q \approx 0.45q_0$, leading to abrupt changes of the order parameters and CM momenta before and after $h_B \approx \Delta_0$. Moreover, we plot the singlet correlation when $h_B > \Delta_0$ in Fig. 3(c). In comparison with the two complete circles of singlet correlations at $h_B < \Delta_0$ [Fig. 3(b)], in the case with $h_B > \Delta_0$ [Fig. 3(c)], the inner circle (type II pairing) is broken around k_z axis whereas the outer circle (type I pairing) survives since the CM momentum is along the favorable orientation to type I pairing (Sec. III A). The appeared regions with the destroyed singlet correlations in this situation, known as the unpairing ones, are the hallmark of the emergence of the FFLO state.[31]

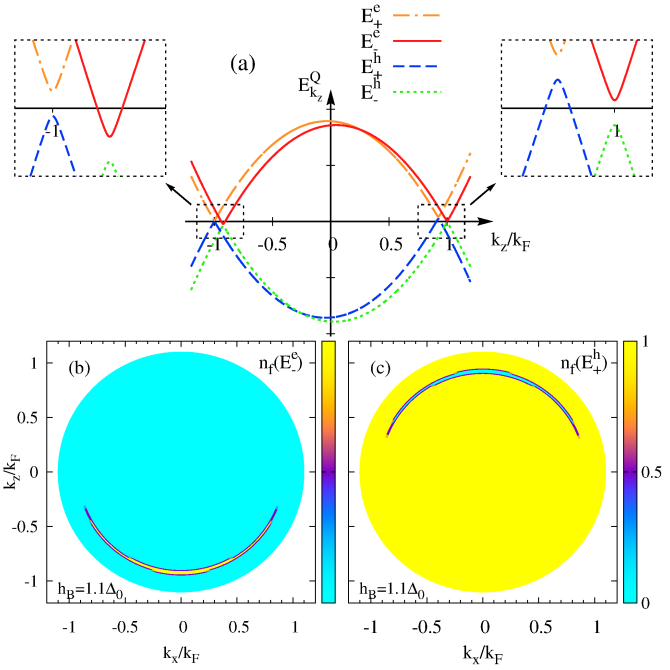

FIG. 4: (a): quasiparticle electron and hole energy spectra along k_z direction; (b) [(c)]: distribution of the quasiparticle electron $n_f(E^e_{-\mathbf{k}})$ [hole $n_f(E^h_{+\mathbf{k}})$] in the momentum space at $h_B = 1.1\Delta_0$. It is also found that $n_f(E^e_{+\mathbf{k}}) = 0$ and $n_f(E^h_{-\mathbf{k}}) = 1$ in the momentum space.

The destruction mechanism of the singlet correlation for the inner circle around k_z axis can be understood as follows in a special direction. With the induced CM momentum pointing to k_z direction (in Sec. III A), along k_z, one has $\mathbf{h_k} = \gamma(k_x, k_y, k_z) = \gamma(0, 0, k_z)$ where the spin-flip terms of the SOC are zero, and then the singlet correlation can be simplified into

$$\rho^s_{\mathbf{q}}(\mathbf{k}) = \mathrm{Tr}\left\{\frac{2\Delta_{\mathbf{q}}[n_f(E^h_{\sigma_3\mathbf{k}}) - n_f(E^e_{\sigma_3\mathbf{k}})]}{\sqrt{(\xi_k + \sigma_3\gamma k_z)^2 + |\Delta_{\mathbf{q}}|^2}}\right\}. \quad (20)$$

Here, the quasiparticle electron and hole energy spectra are written as:

$$E^e_{\sigma_3 k\mathbf{z}} = \sqrt{(\xi_k + \sigma_3\gamma k_z)^2 + |\Delta_{\mathbf{q}}|^2} + \frac{k_z q}{m^*} + \mu\Omega_{q\mathbf{z}}, \quad (21)$$

$$E^h_{\sigma_3 k\mathbf{z}} = -\sqrt{(\xi_k + \sigma_3\gamma k_z)^2 + |\Delta_{\mathbf{q}}|^2} + \frac{k_z q}{m^*} + \mu\Omega_{q\mathbf{z}}. \quad (22)$$

which are plotted Fig. 4(a). When $k_z > 0$, the maximum of factor $\Delta_{\mathbf{q}}/\sqrt{(\xi_k + \sigma_3\gamma k_z)^2 + |\Delta_{\mathbf{q}}|^2}$ occurs at large (small) k_z for $\sigma_3 = -1$ ($\sigma_3 = 1$) in the summation of Eq. (20). Hence, $\sigma_3 = -1$ ($\sigma_3 = 1$) makes the main contribution to the outer (inner) circle of the singlet correlation, e.g., type I (II) pairing, in accord with the pairing spin-down electron 4 (spin-up one 3) in Fig. 2.

In this case, for $\sigma_3 = -1$, as shown in Fig. 4(a), one always has $E^e_- > 0$ (red solid curve) and $E^h_- < 0$ (green dotted curve), and hence $n_f(E^h_{-\mathbf{k}}) - n_f(E^e_{-\mathbf{k}}) = 1$, leading to the finite $\rho^s_{\mathbf{q}}$ for the outer circle. Whereas, for $\sigma = 1$, there exists the region where the quasiparticle hole energy is larger than zero ($E^h_+ > 0$) when $k_z > 0$, as shown by blue dashed curve. This is due to the induced CM momentum, similar to the conventional FFLO state.[31] Together with $E^e_+ > 0$ (brown chain curve), one has $n_f(E^h_{+\mathbf{k}}) - n_f(E^e_{+\mathbf{k}}) = 0$ in this region, leading to the open inner circle of the singlet correlation and hence depairing effect of Cooper pair.

By using the similar analysis, the case with $k_z < 0$ can also be understood. The Fermi distributions of quasiparticle electron and hole in the entire momentum space are plotted in Figs. 4(b) and (c) from full numerical results, respectively. It is found there exist two arc regions with either quasiparticle electron energy below zero or quasiparticle hole one larger than zero, which exactly correspond to the regions with vanishing singlet correlation for the inner circle shown in Fig. 3(c), in consistence with the analysis above.

Furthermore, it is noted that the emerged FFLO state in our work corresponds to the gapless one mentioned in the introduction,[75–78] since the gapless quasiparticle energy spectra $|E^{e/h}_{\mathbf{k}}| = 0$ revealed in the gapless FFLO state[75–77] indicate the emergence of the unpairing regions. By the detailed study of the SOC dependence (refer to Appendix), enhanced Pauli limit and hence enlarged magnetic-field regime of the emerged FFLO state by the SOC is also observed in our work. We further show that this enhancement of the Pauli limit is due to the spin-flip terms of the SOC, which suppress the unpairing regions (also addressed in Appendix).

C. Triplet Correlation and Cooper-Pair Spin Polarization

In this section, by studying the induced p-wave triplet correlations in the pairing regions thanks to the broken space-inversion symmetry by SOC, we show that the Cooper-pair spin polarization,[2,3,94,95] which is predicted to be induced by the magnetic field and CM momentum,[95] exhibits totally different magnetic-field dependences in the drift-BCS and FFLO states due to the abrupt changes of the order parameters and CM momenta. This provides a scheme to experimentally distinguish these two phases through the reported magnetoelectric Andreev effect,[94–96] in addition to the phase transition.

1. *Triplet Correlation*

We first discuss the triplet correlations. Specifically, with the broken space-inversion symmetry by the SOC, p-wave triplet correlations are induced, plotted in Fig. 5

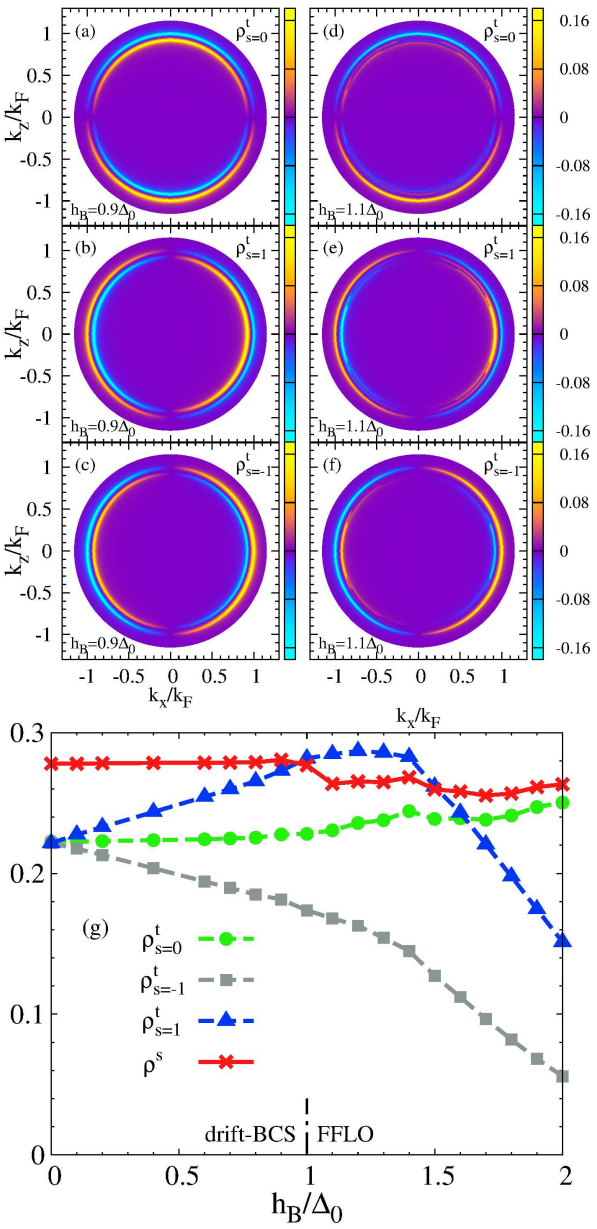

FIG. 5: (a)-(f): momentum dependence of $\rho^t_{s=0}$ and $\rho^t_{s=\pm1}$ in the drift-BCS state at $h_B = 0.9\Delta_0$ and FFLO one at $h_B = 1.1\Delta_0$ correspondingly. (g): maxima of the singlet and triplet correlations in the momentum space as function of h_B. The vertical chain line in (g) indicates the crossover between the drift-BCS and FFLO states.

at different magnetic fields. From the figure, it is seen that in the drift-BCS state ($h_B < \Delta_0$), two separated and complete circles with finite $\rho^t_{s=0}$ [Fig. 5(a)], $\rho^t_{s=1}$ [Fig. 5(b)] and $\rho^t_{s=-1}$ [Fig. 5(c)] are observed in the momentum space, similar to the singlet case [Fig 3(b)]. Moreover, for either the outer or the inner circle, it is seen that the triplet correlations show the p-wave characters: $\rho^t_{s=0} \propto h_{\mathbf{k}z}$ and $\rho^t_{s=\pm1} \propto i h_{\mathbf{k}y} \mp h_{\mathbf{k}x}$, in agreement with the previous works.[4,7,11,12] As for the FFLO state

($h_B > \Delta_0$), as shown in Figs. 5(d), (e) and (f), the inner circles of the triplet correlations are open, similar to the singlet case [Fig 3(c)]. Then, the triplet correlations are only observed in the pairing regions, resembling our previous work.[12]

The magnetic-field dependences of the maximum of the singlet and triplet correlations in the momentum space are plotted in Fig. 5(g). From the figure, it is seen that in either the drift-BCS state ($h_B < \Delta_0$) or the FFLO one ($h_B > \Delta_0$), $\rho^t_{s=0}$ (dashed curve with dots) and $\rho^t_{s=1}$ (dashed curve with triangles) are comparable to the singlet one (solid curve with crosses) when $h_B < 1.7\Delta_0$. Moreover, it is also noted that $\rho^t_{s=1} \neq \rho^t_{s=-1}$ when $h_B \neq 0$, indicating the generation of the Cooper-pair spin polarization by the magnetic field and CM momentum, as predicted in the previous work by Tkachov.[95]

Nevertheless, even with the large p-wave triplet correlations (compared with the singlet one) and the generation of the Cooper-pair spin polarization, the p-wave spin-polarized superfluid is still absent, because of the vanishing p-wave triplet order parameter:

$$\Delta^t(\mathbf{k}) = \sum_{\mathbf{k}'} V_{\mathbf{k}-\mathbf{k}'}\rho^t(\mathbf{k}'), \tag{23}$$

by the s-wave attractive potential $V_{\mathbf{k}-\mathbf{k}'} = V$ and p-wave character: $\rho^t(\mathbf{k}') = -\rho^t(-\mathbf{k}')$. However, it is proposed recently in ultracold atom systems[104,105] that in the presence of the triplet correlation, one can rapidly introduces $\mathbf{k}$-dependent attractive potential $V_{\mathbf{k}-\mathbf{k}'}$ through the Feshbach resonance, and then non-vanishing p-wave superfluid is immediately obtained, at least just after the introduction of the potential. With this approach, the p-wave spin-polarized superfluid can be expected in the spin-orbit coupled ultracold atom systems with a magnetic field, according to our results and analysis above.

2. *Cooper-Pair Spin Polarization*

Next, we show that due to the abrupt changes in order parameters and CM momenta between the drift-BCS and FFLO states, the induced Cooper-pair spin polarizations mentioned in Sec. III C 1, exhibit totally different magnetic-field dependences in these two phases.

Specifically. as mentioned in Sec. III C 1, with the induced triplet correlation, the Cooper-pair spin polarizations, defined as[2,3,94,95]

$$P_c(\mathbf{k}) = |\rho^t_{s=1}(\mathbf{k})|^2 - |\rho^t_{s=-1}(\mathbf{k})|^2, \tag{24}$$

are induced by the magnetic field, plotted in Fig. 6 at different magnetic fields. As seen from the figure, in the drift-BCS state [Fig. 6(a)] and pairing regions of the FFLO one [Fig. 6(b)], it is seen that $P_c(\mathbf{k}) \propto k_x^2$, which can be understood from Eq. (14). Specifically, from Eqs. (14) and (24), one has

$$P_c(\mathbf{k}) \propto |f_{\uparrow\uparrow}(0,\mathbf{k})|^2 - |f_{\downarrow\downarrow}(0,\mathbf{k})|^2 = i\mathbf{f}^t_{\mathbf{q}}(0,\mathbf{k}) \times \mathbf{f}^{t\,*}_{\mathbf{q}}(0,\mathbf{k})|_z. \tag{25}$$

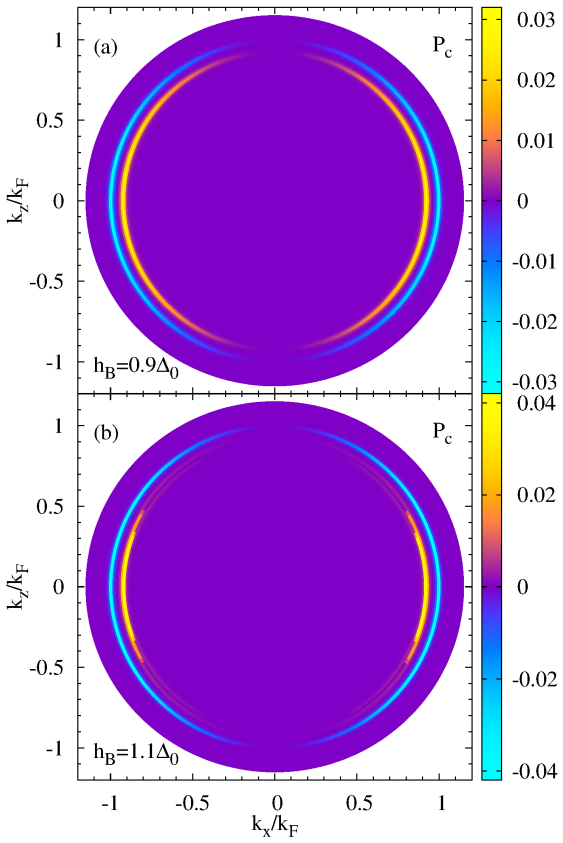

FIG. 6: Momentum dependence of Cooper-pair spin polarization in (a) the drift-BCS state at $h_B = 0.9\Delta_0$ and (b) FFLO one at $h_B = 1.1\Delta_0$.

Then, from Eq. (11), one immediately finds that

$$P_c(\mathbf{k}) \propto [\mathbf{h_k} \times (\mathbf{h_k} \times \mathbf{\Omega_q})]_z |\Delta_\mathbf{q}|^2 = (h^2_{\mathbf{k}x} + h^2_{\mathbf{k}y})\Omega_{q\mathbf{z}}|\Delta_\mathbf{q}|^2, \tag{26}$$

in accord with the numerical results (Fig. 6).

The magnetic-field dependence of the maximum of the Cooper-pair spin polarization $P_c^{\max}$ in the momentum space is plotted in Fig. 7. As seen from the figure, with the increase of h_B, in comparison with the linear increase of $P_c^{\max}$ in the drift-BCS state ($h_B < \Delta_0$), *nonlinear* increase of $P_c^{\max}$ is observed in the FFLO one when $h_B < 1.5\Delta_0$. The totally different magnetic-field dependences of the Cooper-pair spin polarization before and after the phase transition at $h_B = \Delta_0$ provide a scheme to experimentally distinguish the drift-BCS and FFLO states through the reported magnetoelectric Andreev effect,[94–96] in addition to the phase transition. Moreover, by further increasing the magnetic field after $1.5\Delta_0$, it is seen that $P_c^{\max}$ markedly decreases and hence a peak, as a unique feature of the FFLO state, is observed.

From Eq. (26), the magnetic-field dependence of $P_c^{\max}$ can be clearly understood. Specifically, in the drift-BCS states ($h_B < \Delta_0$), with $\Omega_{q\mathbf{z}} \approx h_B$ and the marginal variation of $\Delta_\mathbf{q}$ [Fig. 3(a)], $P_c^{\max}$ increases linearly with

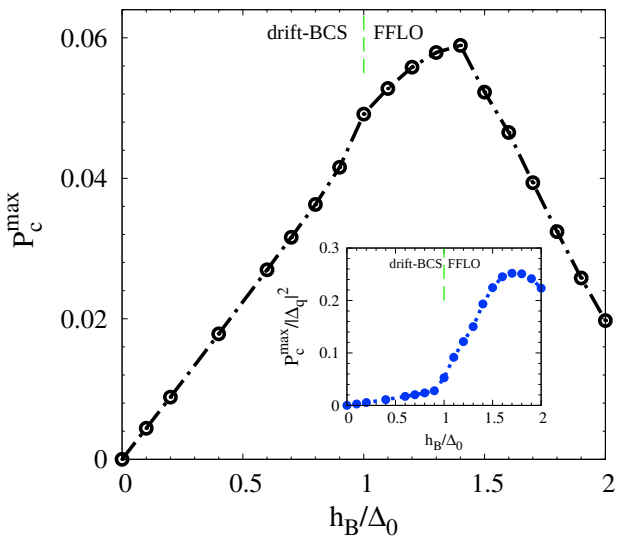

FIG. 7: Maximum of Cooper-pair spin polarization in the momentum space versus magnetic field. The inset shows $P_c^{\max}/|\Delta_{\mathbf{q}}|^2$ as function of h_B. The vertical dashed line indicates the crossover between the drift-BCS and FFLO states.

h_B. As for the FFLO state, with the increase of h_B at $\Delta_0 < h_B < 1.5\Delta_0$, although $\Delta_{\mathbf{q}}$ is suppressed [Fig. 3(a)], $\Omega_{q\mathbf{z}}$ ($\propto= h_B + h_{q\mathbf{z}}$) is markedly enhanced due to the increased CM momentum $\mathbf{q}$ [inset (I) of Fig. 3(a)]. By the stronger enhancement from $\Omega_{q\mathbf{z}}$ than the suppression from $|\Delta_{\mathbf{q}}|^2$ in Eq. (26) at $\Delta_0 < h_B < 1.5\Delta_0$, $P_c^{\max}$ increases nonlinearly with h_B. This can be justified by plotting $P_c^{\max}/|\Delta_{\mathbf{q}}|^2$ ($\propto \Omega_{q\mathbf{z}}$) versus h_B in the inset of Fig. 7, from which it is seen that $P_c^{\max}/|\Delta_{\mathbf{q}}|^2$ is markedly enhanced at $\Delta_0 < h_B < 1.5\Delta_0$. By further increasing h_B after $1.5\Delta_0$, $\mathbf{q}$ becomes saturated at $0.47q_0\mathbf{z}$ [inset (I) of Fig. 3(a)], and hence the suppression of $\Delta_{\mathbf{q}}$ leads to the marked decrease of $P_c^{\max}$.

IV. SUMMARY

In summary, we have systematically investigated the properties of the FFLO state with an induced CM momentum in the spin-orbit-coupled superconductor Li_2Pd_3B in the presence of the magnetic field. Differing from the previous theoretical works[74–78] where the study is based on the numerical calculation of the free-energy minimum with respect to the CM momentum and order parameter, in our work, by analytically obtaining the anomalous Green function and hence the gap equation, the superconducting state can be determined by computing the energy minimum with respect to a single parameter, i.e., the CM momentum. Moreover, from the obtained anomalous Green function, properties of the superconducting state including quasiparticle energy spectra, singlet and triplet correlations, behaviors of the CM momentum and order parameter at the phase transition are also addressed in our work.

Specifically, it is found that with the SOC, the CM momentum parallel to the magnetic field is induced at small magnetic field, similar to the gapped FFLO state in the previous works.[75–78] Nevertheless, we have shown that two complete circles of the singlet correlation due to the SOC are observed in the momentum space, and no unpairing region with vanishing singlet correlation appears. This is very different from the conventional FFLO state without SOC, where the CM momentum is induced simultaneously with the emergence of the unpairing regions.[31] By further studying the pairing mechanism, it is shown that the induced CM momentum with SOC at small magnetic field is due to the energy-spectrum distortion, resembling the intravalley pairing in graphene[92] and transition metal dichalcogenides,[93] and hence has different origin from the case in conventional FFLO state.[31] Therefore, it is more appropriate to refer to such superconducting state, in which the CM momentum is induced but no unpairing region is developed, as the drift-BCS state. By further increasing the magnetic field, abrupt enhancement of the CM momenta and suppression on the order parameters are observed, indicating the occurrence of the first-order phase transition. Particularly, we find that open circle of the singlet correlation, i.e., unpairing region with vanishing singlet correlation, is induced after the phase transition, showing the emergence of the FFLO state. It is further shown that induced unpairing regions arises from the quasiparticle electron and hole with energies below and larger than zero, respectively, indicating the emerged FFLO state here corresponds to the gapless one in the previous works.[75–78] Enhanced Pauli limit and hence enlarged magnetic-field regime of the emerged FFLO state are also observed in our work, and we demonstrate that the enhancement of the Pauli limit is due to the spin-flip terms of the SOC, which suppress the unpairing regions.

Finally, we discuss the triplet correlation induced by the SOC, and show that in the presence of the triplet correlation, the Cooper-pair spin polarizations,[2,3,94,95] induced by the magnetic field and CM momentum, exhibit totally different magnetic-field dependences between the drift-BCS and FFLO states. This difference between the drift-BCS and FFLO states, arising from the abrupt changes in order parameters and CM momenta, provides a scheme to experimentally distinguish these two phases through the reported magnetoelectric Andreev effect,[94–96] in addition to the phase transition.

Appendix A: SOC DEPENDENCE

In this part, we address the SOC dependence of the superconducting state. The magnetic field dependences of the order parameter $\Delta_{\mathbf{q}}$ and CM momentum $\mathbf{q} = q\mathbf{z}$ are plotted in Fig. 8(a) and the inset of the same figure at different SOCs, respectively. As seen from the figure, with the increase of the SOC strength, the Pauli limit is enhanced and hence the regime where the FFLO occurs

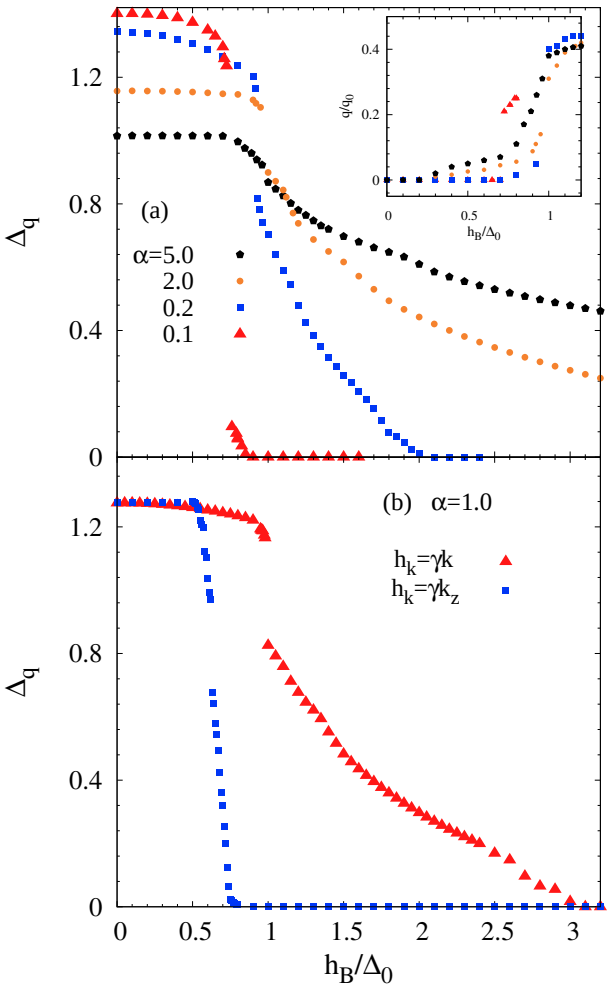

FIG. 8: (a): $\Delta_{\mathbf{q}}$ versus h_B at different SOCs. The inset shows $\mathbf{q} = q\mathbf{z}$ as function of h_B at different SOCs. In the calculation, $\gamma = \alpha\gamma_0$ with γ_0 being the SOC strength in Li_2Pd_3B. (b): $\Delta_{\mathbf{q}}$ versus h_B at $\alpha = 1$. Triangles (Squares) in (b): the spin-flip terms of the SOC are included (removed) by setting $\mathbf{h_k} = \gamma\mathbf{k}$ ($\mathbf{h_k} = \gamma k_z\mathbf{z}$).

is enlarged, in accord with the previous experiments[82–85] and prediction.[74]

The enhancement of the Pauli limit is due to the spin-flip terms of the SOC (perpendicular to $\mathbf{h}_B$). This can be seen from Fig. 8(b) where we plot $\Delta_{\mathbf{q}}$ versus h_B with and without the spin-flip terms of the SOC. From the figure, it is seen that in comparison with the case at $\mathbf{h_k} = \gamma\mathbf{k}$ (triangles), in the situation without the spin-flip terms of the SOC ($\mathbf{h_k} = \gamma k_z\mathbf{z}$), as shown by squares, the Pauli limit is markedly suppressed and the FFLO state occurs in a narrow magnetic-field regime. This is because that away from the k_z axis, the spin-flip terms of the SOC couple the quasiparticle electrons $E^e_{+\mathbf{k}}$ and $E^e_{-\mathbf{k}}$ (holes $E^h_{+\mathbf{k}}$ and $E^h_{-\mathbf{k}}$) with different spin polarizations in Fig. 4(a). Consequently, due to $E^e_{+\mathbf{k}} > 0$ ($E^h_{-\mathbf{k}} < 0$) shown in Fig. 4(a), the regions with $E^e_{-\mathbf{k}} < 0$ ($E^h_{+\mathbf{k}} > 0$) mentioned in Sec. III B, i.e., the unpairing regions, are suppressed, leading to the suppressed Pauli limit.

Furthermore, it is noted that at very small SOC $\gamma = 0.1\gamma_0$ (shown by triangles), the FFLO state occurs in a narrow regime $0.7\Delta_0 < h_B < 0.8\Delta_0$, close to the conventional FFLO one without SOC ($0.66\Delta_0 < h_B < 0.8\Delta_0$).[31] With the increase of the SOC, the variation of $\Delta_{\mathbf{q}}$ at the phase transition between the drift-BCS and FFLO states is suppressed. Particularly, when we extend to a large SOC $\gamma = 5\gamma_0$ [shown by pentagons in Fig. 8(a)], the variation of $\Delta_{\mathbf{q}}$ at the phase transition ($h_B = \Delta_0$) becomes nearly indistinguishable but still exists. This case is very similar to Fig. 4(b) in Ref. 75. This suppressed variation of $\Delta_{\mathbf{q}}$ at the phase transition is due to the enhancement of the CM momentum in the drift-BCS state by the SOC, leading to the close CM momenta between the drift-BCS ($h_B < \Delta_0$) and FFLO ($h_B > \Delta_0$) states, as shown by pentagons in the inset of Fig. 8(a).

Nevertheless, with the larger SOC $\gamma > 5\gamma_0$ ($\Delta_0 \ll \gamma k_F$), the mean-field theory $\Delta_{\mathbf{q}} = -V\sum'_{\mathbf{k}}\langle\phi_{\uparrow\mathbf{k}+\mathbf{q}}\phi_{\downarrow-\mathbf{k}+\mathbf{q}}\rangle$ in colinear space is inappropriate due to the large spin-flip terms of the SOC. In this case, pairing mechanism and the generation of the CM momentum should be discussed in the helix space, which is beyond the scope of our work.

* Author to whom correspondence should be addressed; Electronic address: mwwu@ustc.edu.cn.

1 J. Bardeen, L. N. Cooper, and J. R. Schrieffer, Phys. Rev. **106**, 162 (1957).
2 A. J. Leggett, Rev. Mod. Phys. **47**, 331 (1975).
3 M. Sigrist and K. Ueda, Rev. Mod. Phys. **63**, 239 (1991).
4 L. P. Gor'kov and E. I. Rashba, Phys. Rev. Lett. **87**, 037004 (2001).
5 P. A. Frigeri, D. F. Agterberg, A. Koga, and M. Sigrist, Phys. Rev. Lett. **92**, 097001 (2004).
6 Z. H. Yang, J. Wang, and K. S. Chan, Supercond. Sci. Technol. **22**, 055012 (2009).
7 E. Bauer and M. Sigrist, *Non-centrosymmetric Superconductors: Introduction and Overview* (Springer Science and Business Media, Berlin, 2012).
8 X. Liu, J. K. Jain, and C. X. Liu, Phys. Rev. Lett. **113**, 227002 (2014).
9 C. R. Reeg and D. L. Maslov, Phys. Rev. B **92**, 134512 (2015).
10 C. Triola, D. M. Badiane, A. V. Balatsky, and E. Rossi, Phys. Rev. Lett. **116**, 257001 (2016).
11 T. Yu and M. W. Wu, Phys. Rev. B **93**, 195308 (2016).
12 F. Yang and M. W. Wu, Phys. Rev. B **95**, 075304 (2017).
13 P. W. Anderson and W. F. Brinkman, Phys. Rev. Lett. **30**, 1108 (1973).
14 W. F. Brinkman, J. W. Serene, and P. W. Anderson, Phys. Rev. A **10**, 2386 (1974).
15 T. M. Rice and M. Sigrist, J. Phys. Condens. Matter **7**,

L643 (1995).
[16] Y. Maeno, H. Hashimoto, K. Yoshida, S. Nishizaki, T. Fujita, J. G. Bednorz, and F. Lichtenberg, Nature (London) **372**, 532 (1994).
[17] K. Ishida, Y. Kitaoka, K. Asayama, S. Ikeda, S. Nishizaki, Y. Maeno, K. Yoshida, and T. Fujita, Phys. Rev. B **56**, R505(R) (1997).
[18] N. Read and D. Green, Phys. Rev. B **61**, 10267 (2000).
[19] D. A. Ivanov, Phys. Rev. Lett. **86**, 268 (2001).
[20] A. P. Mackenzie and Y. Maeno, Rev. Mod. Phys. **75**, 657 (2003).
[21] R. Meservey and P. M. Tedrow, Phys. Rep. **238**, 173 (1994).
[22] *Semiconductor Spintronics and Quantum Computation*, edited by D. D. Awschalom, D. Loss, and N. Samarth (Springer, Berlin, 2002).
[23] I. Žutić, J. Fabian, and S. D. Sarma, Rev. Mod. Phys. **76**, 323 (2004).
[24] A. I. Buzdin, Rev. Mod. Phys. 77, 935 (2005).
[25] F. S. Bergeret, A. F. Volkov, and K. B. Efetov, Rev. Mod. Phys. **77**, 1321 (2005).
[26] J. Fabian, A. M. Abiague, C. Ertler, P. Stano, and I. Žutić, Acta Phys. Slov. **57**, 565 (2007).
[27] M. W. Wu, J. H. Jiang, and M. Q. Weng, Phys. Rep. **493**, 61 (2010).
[28] *Handbook of Spin Transport and Magnetism*, edited by E. Y. Tsymbal and I. Žutić (CRC, Boca Raton, FL, 2011).
[29] M. Eschrig, Phys. Today **64**(1), 43 (2011).
[30] J. Linder and J. W. A. Robinson, Nat. Phys. **11**, 307 (2015).
[31] P. Fulde and A. Ferrell, Phys. Rev. **135**, A550 (1964).
[32] A. I. Larkin and Y. N. Ovchinnikov, Sov. Phys. JETP **20**, 762 (1965) [Zh. Eksp. Teor. Fiz. **47**, 1136 (1964)].
[33] K. Maki, Phys. Rev. **148**, 362 (1966).
[34] L. Gruenberg and L. Gunther, Phys. Rev. Lett. **16**, 996 (1966).
[35] H. A. Radovan, N. A. Fortune, T. P. Murphy, S. T. Hannahs, E. C. Palm, S. W. Tozer, and D. Hall, Nature **425**, 51 (2003).
[36] A. Bianchi, R. Movshovich, C. Capan, P. G. Pagliuso, and J. L. Sarrao, Phys. Rev. Lett. **91**, 187004 (2003).
[37] C. Capan, A. Bianchi, R. Movshovich, A. D. Christianson, A. Malinowski, M. F. Hundley, A. Lacerda, P. G. Pagliuso, and J. L. Sarrao, Phys. Rev. B **70**, 134513 (2004).
[38] T. Watanabe, Y. Kasahara, K. Izawa, T. Sakakibara, Y. Matsuda, C. J. van der Beek, T. Hanaguri, H. Shishido, R. Settai, and Y. Onuki, Phys. Rev. B **70**, 020506 (2004).
[39] K. Kakuyanagi, M. Saitoh, K. Kumagai, S. Takashima, M. Nohara, H. Takagi, and Y. Matsuda, Phys. Rev. Lett. **94**, 047602 (2005).
[40] K. Kumagai, M. Saitoh, T. Oyaizu, Y. Furukawa, S. Takashima, M. Nohara, H. Takagi, and Y. Matsuda, Phys. Rev. Lett. **97**, 227002 (2006).
[41] V. F. Mitrovic, M. Horvatic, C. Berthier, G. Knebel, G. Lapertot, and J. Flouquet, Phys. Rev. Lett. **97**, 117002 (2006).
[42] Y. Matsuda and H. Shimahara, J. Phys. Soc. Jpn. **76**, 051005 (2007).
[43] M. Kenzelmann, S. Gerber, N. Egetenmeyer, J. L. Gavilano, Th. Strässle, A. D. Bianchi, E. Ressouche, R. Movshovich, E. D. Bauer, J. L. Sarrao, and J. D. Thompson, Phys. Rev. Lett. **104**, 127001 (2010).
[44] R. Casalbuoni and G. Nardulli, Rev. Mod. Phys. **76**, 263 (2004).
[45] T. Mizushima, K. Machida, and M. Ichioka, Phys. Rev. Lett. **94**, 060404 (2005).
[46] M. W. Zwierlein, A. Schirotzek, C. H. Schunck, and W. Ketterle, Science **311**, 492 (2006).
[47] D. E. Sheehy and L. Radzihovsky, Phys. Rev. Lett. **96**, 060401 (2006).
[48] M. M. Parish, S. K. Baur, E. J. Mueller, and D. A. Huse, Phys. Rev. Lett. **99**, 250403 (2007).
[49] T. K. Koponen, T. Paananen, J. P. Martikainen, and P. Törmä, Phys. Rev. Lett. **99**, 120403 (2007).
[50] Y. A. Liao, A. S. C. Rittner, T. Paprotta, W. Li, G. B. Partridge, R. G. Hulet, S. K. Baur, and E. J. Mueller, Nature (London) **467**, 567 (2010).
[51] F. Chevy and C. Mora, Rep. Prog. Phys. **73**, 112401 (2010).
[52] Z. Cai, Y. Wang, and C. Wu, Phys. Rev. A **83**, 063621 (2011).
[53] A. Gurevich, Phys. Rev. B **82**, 184504 (2010).
[54] K. Cho, H. Kim, M. A. Tanatar, Y. J. Song, Y. S. Kwon, W. A. Coniglio, C. C. Agosta, A. Gurevich, and R. Prozorov, Phys. Rev. B **83**, 060502(R) (2011).
[55] S. Khim, B. Lee, J. W. Kim, E. S. Choi, G. R. Stewart, and K. H. Kim, Phys. Rev. B **84**, 104502 (2011).
[56] A. Gurevich, Rep. Prog. Phys. **74**, 124501 (2011).
[57] H. Shimahara, J. Phys. Soc. Jpn. **66**, 541 (1997).
[58] M. A. Tanatar, T. Ishiguro, H. Tanaka, and H. Kobayashi, Phys. Rev. B **66**, 134503 (2002).
[59] S. Uji, T. Terashima, M. Nishimura, Y. Takahide, T. Konoike, K. Enomoto, H. Cui, H. Kobayashi, A. Kobayashi, H. Tanaka, M. Tokumoto, E. S. Choi, T. Tokumoto, D. Graf, and J. S. Brooks, Phys. Rev. Lett. **97**, 157001 (2006).
[60] R. Lortz, Y. Wang, A. Demuer, P. H. M. Böttger, B. Bergk, G. Zwicknagl, Y. Nakazawa, and J. Wosnitza, Phys. Rev. Lett. **99**, 187002 (2007).
[61] B. Bergk, A. Demuer, I. Sheikin, Y. Wang, J. Wosnitza, Y. Nakazawa, and R. Lortz, Phys. Rev. B **83**, 064506 (2011).
[62] J. A. Wright, E. Green, P. Kuhns, A. Reyes, J. Brooks, J. Schlueter, R. Kato, H. Yamamoto, M. Kobayashi, and S. E. Brown, Phys. Rev. Lett. **107**, 087002 (2011).
[63] R. Beyer and J. Wosnitza, Low Temp. Phys. **39**, 225 (2013).
[64] H. Mayaffre, S. Krämer, M. Horvatic, C. Berthier, K. Miyagawa, K. Kanoda, and V. V. Mitrovic, Nat. Phys. **10**, 928 (2014).
[65] L. G. Aslamazov, Sov. Phys. JETP **28**, 773 (1969) [Zh. Eksp. Teor. Fiz. **55**, 1477 (1968)].
[66] S. Takada, Prog. Theor. Phys. **43**, 27 (1970).
[67] L. W. Gruenberg and L. Gunther, Phys. Rev. Lett. **16**, 996 (1966).
[68] H. Adachi and R. Ikeda, Phys. Rev. B **68**, 184510 (2003).
[69] H. Shimahara, Phys. Rev. B **50**, 12760 (1994).
[70] G. Dresselhaus, Phys. Rev. **100**, 580 (1955).
[71] Y. A. Bychkov and E. I. Rashba, J. Phys. C **17**, 6039 (1984).
[72] Y. A. Bychkov, JETP Lett. **39**, 78 (1984).
[73] L. Dong, L. Jiang, H. Hu, and J. Pu, Phys. Rev. A **87**, 043616 (2013).
[74] Z. Zheng, M. Gong, X. Zou, C. Zhang, and G. C. Guo, Phys. Rev. A **87**, 031602 (2013).
[75] L. Dong, L. Jiang, and H. Pu, New J. Phys. **15**, 075014

(2013).
[76] X. J. Liu and H. Hu, Phys. Rev. A **87**, 051608(R) (2013).
[77] F. Wu, G. C. Guo, W. Zhang, and W. Yi, Phys. Rev. Lett. **110**, 110401 (2013).
[78] X. F. Zhou, G. C. Guo, W. Zhang, and W. Yi, Phys. Rev. A **87**, 063606 (2013).
[79] C. Chen, Phys. Rev. Lett. **111**, 235302 (2013).
[80] Y. Xu, C. L. Qu, M. Gong, and C. W. Zhang, Phys. Rev. A **89**, 013607 (2014).
[81] G. Zwicknagl, S. Jahns, and P. Fulde, arXiv:1701.09121.
[82] D. Aoki, A. Huxley, E. Ressouche, D. Braithwaite, J. Flouquet, J. P. Brison, E. Lhotel, and C. Paulsen, Nature **413**, 613 (2001).
[83] M. B. Shalom, M. Sachs, D. Rakhmilevitch, A. Palevski, and Y. Dagan, Phys. Rev. Lett. **104**, 126802 (2010).
[84] J. F. Mercure, A. F. Bangura, X. F. Xu, N. Wakeham, A. Carrington, P. Walmsley, M. Greenblatt, and N. E. Hussey, Phys. Rev. Lett. **108**, 187003 (2012).
[85] M. Smidman, M. B. Salamon, H. Q. Yuan, and D. F. Agterberg, Rep. Prog. Phys. **80**, 036501 (2017).
[86] K. W. Lee and W. E. Pickett, Phys. Rev. B **72**, 174505 (2005).
[87] H. Takeya, K. Hirata, K. Yamaura, and K. Togano, M. E. Massalami, R. Rapp, and F. A. Chaves, B. Ouladdiaf, Phys. Rev. B **72**, 104506 (2005).
[88] R. Khasanov, I. L. Landau, C. Baines, F. L. Mattina, A. Maisuradze, K. Togano, and H. Keller, Phys. Rev. B **73**, 214528 (2006).
[89] S. Tsuda, T. Yokoya, T. Kiss, T. Shimojima, K. Ishizaka, S. Shin, T. Togashi, S. Watanabe, C. Q. Zhang, C. T. Chen, I. Hase, H. Takeya, K. Hirata, and K. Togano, J. Phys. Soc. Jpn. **78**, 034711 (2009).
[90] S. P. Mukherjee and T. Takimoto, Phys. Rev. B **86**, 134526 (2012).
[91] H. Q. Yuan, D. F. Agterberg, N. Hayashi, P. Badica, D. Vandervelde, K. Togano, M. Sigrist, and M. B. Salamon, Phys. Rev. Lett. **97**, 017006 (2016).
[92] M. Einenkel and K. B. Efetov, Phys. Rev. B **84**, 214508 (2011).
[93] S. Tsuchiya, J. Goryo, E. Arahata, and M. Sigrist, Phys. Rev. B **94**, 104508 (2016).
[94] A. D. Hillier, J. Quintanilla, B. Mazidian, J. F. Annett, and R. Cywinski, Phys. Rev. Lett. **109**, 097001 (2012).
[95] G. Tkachov, Phys. Rev. Lett. **118**, 016802 (2017).
[96] P. Högl, A. M. Abiague, I. Žutić, and J. Fabian, Phys. Rev. Lett. **115**, 116601 (2015).
[97] A. A. Abrikosov, L. P. Gorkov, and I. E. Dzyaloshinski, *Methods of Quantum Field Theory in Statistical Physics* (Prentice Hall, Englewood Cliffs, NJ, 1963).
[98] A. L. Fetter and J. D. Walecka, *Quantum Theory of Many Particle Systems* (McGraw-Hill, New York, 1971).
[99] G. D. Mahan, *Many Particle Physics* (Plenum, New York, 1990).
[100] L. P. Gorkov, Zh. Eksp. Teor. Fiz. **36**, 1918 (1959) [Sov. Phys. JETP **9**, 1364 (1959)]; Zh. Eksp. Teor. Fiz. **37**, 1407 (1959) [Sov. Phys. JETP **10**, 998 (1960)].
[101] G. Annunziata, D. Manske, and J. Linder, Phys. Rev. B **86**, 174514 (2012).
[102] D. Fritsch and J. F. Annett, J. Phys. Condens. Matter **26**, 274212 (2014).
[103] T. Yu and M. W. Wu, Phys. Rev. B **94**, 205305 (2016).
[104] Y. Endo, D. Inotani, R. Hanai, and Y. Ohashi, Phys. Rev. A **92**, 023610 (2015).
[105] T. Yamaguchi and Y. Ohashi, Phys. Rev. A. **92**, 013615 (2015).